energies

MDPI

Review

Research Progress in High-Throughput Screening of CO_2 Reduction Catalysts

Qinglin Wu [1], Meidie Pan [2], Shikai Zhang [1], Dongpeng Sun [1], Yang Yang [1], Dong Chen [1,2,3,*], David A. Weitz [4] and Xiang Gao [1,*]

[1] College of Energy Engineering and State Key Laboratory of Clean Energy Utilization, Zhejiang University, Hangzhou 310003, China
[2] Department of Medical Oncology, The First Affiliated Hospital, School of Medicine, Zhejiang University, Hangzhou 310003, China
[3] Zhejiang Key Laboratory of Smart Biomaterials, College of Chemical and Biological Engineering, Zhejiang University, Hangzhou 310027, China
[4] John A. Paulson School of Engineering and Applied Sciences, Harvard University, Cambridge, MA 02138, USA
* Correspondence: chen_dong@zju.edu.cn (D.C.); xgao@zju.edu.cn (X.G.)

Abstract: The conversion and utilization of carbon dioxide (CO_2) have dual significance for reducing carbon emissions and solving energy demand. Catalytic reduction of CO_2 is a promising way to convert and utilize CO_2. However, high-performance catalysts with excellent catalytic activity, selectivity and stability are currently lacking. High-throughput methods offer an effective way to screen high-performance CO_2 reduction catalysts. Here, recent advances in high-throughput screening of electrocatalysts for CO_2 reduction are reviewed. First, the mechanism of CO_2 reduction reaction by electrocatalysis and potential catalyst candidates are introduced. Second, high-throughput computational methods developed to accelerate catalyst screening are presented, such as density functional theory and machine learning. Then, high-throughput experimental methods are outlined, including experimental design, high-throughput synthesis, in situ characterization and high-throughput testing. Finally, future directions of high-throughput screening of CO_2 reduction electrocatalysts are outlooked. This review will be a valuable reference for future research on high-throughput screening of CO_2 electrocatalysts.

Keywords: CO_2 reduction; electrocatalyst; high-throughput computing; machine learning; high-throughput screening; in situ characterization

Citation: Wu, Q.; Pan, M.; Zhang, S.; Sun, D.; Yang, Y.; Chen, D.; Weitz, D.A.; Gao, X. Research Progress in High-Throughput Screening of CO_2 Reduction Catalysts. *Energies* **2022**, *15*, 6666. https://doi.org/10.3390/en15186666

Academic Editors: Rafael Estevez, Vicente Montes and Manuel Checa

Received: 3 August 2022
Accepted: 5 September 2022
Published: 13 September 2022

1. Introduction

With the development of the economy and the rising global population, energy demand has surged year by year. Currently, most energy is from fossil fuels, which leads to the emission of a large amount of CO_2 [1,2]. CO_2 is among the leading greenhouse gases that cause global warming and thus great harm to the global ecological environment. Meanwhile, CO_2 is an important carbon source for producing many chemicals and fuels, such as carbon monoxide, methanol, methane, formic acid, oxalic acid, formaldehyde, and so on [3–9]. Therefore, converting CO_2 into energy substances and chemical feedstocks plays a vital role in reducing CO_2 emissions and addressing energy demand.

The utilization of CO_2 as a carbon source is carried out in various ways, such as thermochemical [10–13], photochemical [14–17], electrochemical [18–21], and biochemical methods [22–24]. However, due to the stable chemical structure of CO_2 [25], it is necessary to provide high activation energy or use catalysts to convert CO_2. Catalysts can effectively reduce the activation energy for chemical reactions and promote the reaction under relatively mild conditions, thus decreasing the response's energy consumption. Therefore, high-performance catalysts are critical for CO_2 conversion.

Current research on CO_2 conversion is devoted to the mechanism of CO_2 reduction [26–28] and the search for high-performance CO_2 reduction catalysts with excellent activity, selectivity, and stability [4,29–31]. The indicators used to evaluate the performance of catalysts include product conversion rate, amount of side product, catalyst stability, energy efficiency, and so on [32–34].

Previously, screening of high-performance catalysts is mainly based on trial-and-error learning. Generally, the performance of catalysts is closely related to many parameters, such as catalyst composition, structure, and so on. Therefore, the parameter space for the exploration of high-performance catalysts is so huge that it is difficult to screen out high-performance catalysts using conventional methods [35,36]. In addition, high-throughput screening of CO_2 reduction catalysts still faces the problems of low efficiency, high cost, and insufficient accuracy. To address the problem, high-throughput methods are proposed for the rapid screening of high-performance catalysts.

High-throughput methods make it possible to systematically explore the parameter space and effectively solve the complex problem of exploring the large parameter space by processing a large number of catalyst candidates in parallel at one time, greatly improving the screening efficiency and reducing the screening cost. High-throughput screening of high-performance CO_2 reduction catalysts generally involves four steps, e.g., experimental design, high-throughput synthesis, in situ characterization, and high-throughput testing. A systematic and timely review of high-throughput technologies will facilitate the fast screening of high-performance catalysts for CO_2 conversion.

This paper will review the recent applications of high-throughput technologies and focus on the following four parts: (1) Present the reaction mechanism of CO_2 electrocatalytic reduction and typical catalyst candidates. (2) Introduce the research progress of high-throughput computational methods, such as density functional theory and machine learning. (3) Discuss high-throughput experimental methods, including experimental design, high-throughput synthesis, in situ characterization, and high-throughput testing. (4) Summarize the application prospects of high-throughput methods in screening high-performance catalysts for CO_2 electrocatalytic reduction. Both high-throughput computational and experimental methods are indispensable for high-throughput screening. High-throughput computing could better determine the parameter space for high-throughput experiments, thus improving the screening efficiency. In return, experimental results obtained by high-throughput experiments are able to provide the large data for high-throughput computing and help to improve the accuracy of high-throughput computing. A combined review of high-throughput computational and experimental methods will benefit the development of high-throughput screening.

2. Mechanism of CO_2 Electrocatalytic Reduction

CO_2 can be converted into valuable chemical feedstocks and fuels in various ways, such as thermochemical, photochemical, electrochemical, and biochemical reactions. Among these methods, the electrochemical reaction has the advantages of a changeable electrode, tunable potential, controllable temperature, recoverable electrolyte, clean electric energy supply, and compact structure [37]. Therefore, electrocatalytic reduction is widely used for CO_2 conversion. A typical electrocatalytic system consists of an electrolyte, two electrodes, and a thin membrane between the two electrodes, as shown in Figure 1a [28]. Under an applied potential, CO_2 reduction occurs at the cathode/electrolyte interface; ions and molecules in the electrolytes react with CO_2 at the interface to form various products [28].

CO_2 electrocatalytic reduction is very complex, and the reaction strongly depends on electrolyte, catalyst, applied potential, and temperature [38]. Typical electrolytes for CO_2 electrocatalytic reduction include aqueous solutions, ionic liquids, and organic solvents. The mechanism of CO_2 electrocatalytic reduction in an aqueous solution and the formation pathways of five main C_1 products in the reduction process is shown in Figure 1b [39].

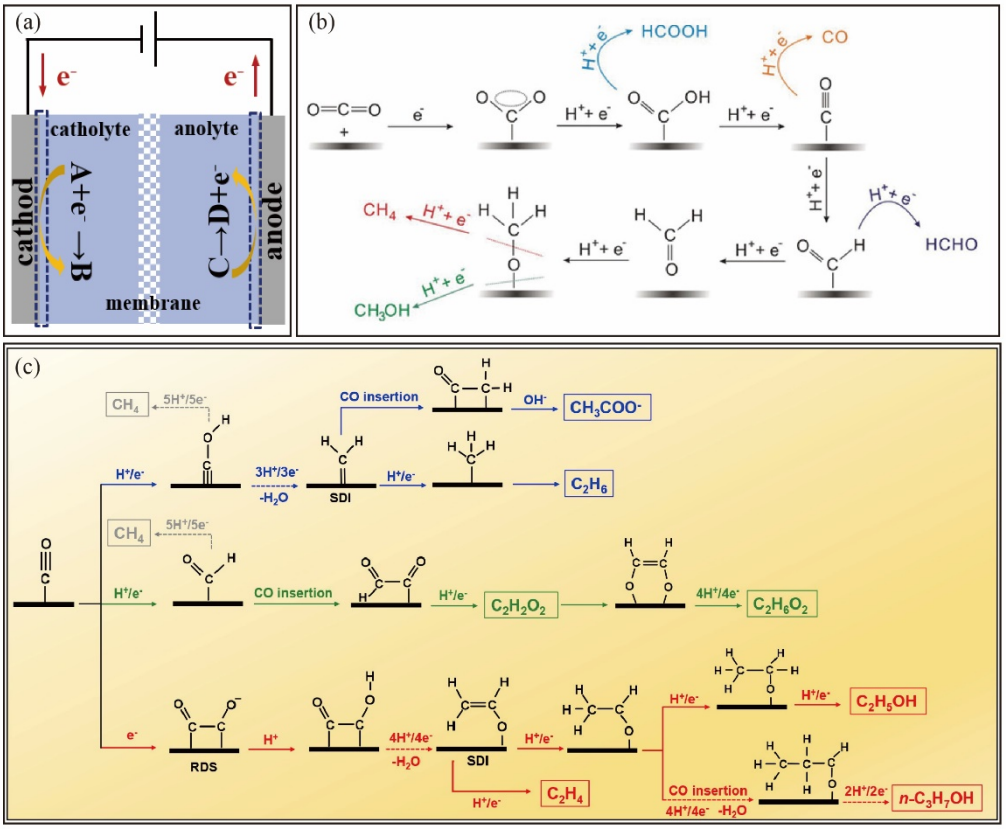

Figure 1. Electrocatalytic system and principle of CO_2 electrocatalytic reaction. (**a**) Model of a typical electrocatalytic system. Reprinted with permission from Ref. [28]. Copyright 2020, Elsevier. (**b**) Mechanism of CO_2 electrocatalytic reduction on electrodes in aqueous solutions. The formation paths of the five main C_1 products are illustrated during the reduction process. Reprinted with permission from Ref. [39]. Copyright 2017, John Wiley and Sons. (**c**) C_2 and C_3 pathways starting from *CO on Cu surfaces. Reprinted with permission from Ref. [40]. Copyright 2019, American Chemical Society.

The catalysts for CO_2 reduction have important influences on product selectivity. Numerous elements and compounds have been developed as catalysts for the electrocatalytic reduction of CO_2, such as Ti, Cr, Mn, Ni, Cu, Pt, Au, and Ag [41–46]. The main products and the corresponding metal elements are summarized in Table 1 [29]. When Ni, Fe, Pt, Ti, Ga, and Co are used as the electrocatalysts for CO_2 reduction, H_2 desorbs more easily from the surface, and thus H_2 is mainly produced [47]. Au, Ag, and Zn have weak adsorption capacity for CO intermediates, thus mainly generating CO. In contrast, Pd, Hg, In, Sn, Cd, Tl, and Bi containing p electrons have stronger adsorption capacity for $CO_2^{\cdot-}$ and mainly produce HCOOH [39]. For Cu, due to the suitable adsorption and desorption capacities between the Cu surface and active intermediates, C−C coupling reaction occurs on the Cu surface in the middle of adsorption, and some high-value-added hydrocarbons, such as methane, are generated [48]. In addition, Cu is a relatively inexpensive metal, showing promising application prospects.

The electrocatalytic reductions of CO_2 on Cu substrate under various electrode potentials have also been investigated, and sixteen different reaction products are detected. Among the sixteen products, C_2 and C_3 products could be obtained through intermediates, such as adsorbed *CO [49–51]. Possible pathways for C_2 and C_3 products starting from *CO on the copper surface are shown in Figure 1c [40].

Table 1. Main products of CO_2 reduction reaction on different catalytic materials. Reprinted with permission from Ref. [29]. Copyright 2016, Elsevier.

Group	Metal Element	Main Product
I	Ni, Fe, Pt, Ti, Ga, Co	H_2
II	Au, Ag, Zn	CO
III	Pd, Hg, In, Sn, Cd, Tl, Bi	HCOOH
IV	Cu	Hydrocarbons/Oxygenates

Among the parameters affecting the electrocatalytic reduction of CO_2, the study of electrocatalysts has dramatically promoted the utilization of CO_2. However, electrocatalytic reduction of CO_2 remains challenging, due to poor product selectivity, low electrocatalyst activity, poor electrocatalyst stability, high energy consumption, and low energy efficiency [52,53]. These challenges severely restrict the electrocatalytic reduction of CO_2.

Many studies have shown that doping different elements to form heterogeneous electrocatalysts, which possess abundant catalytically active sites, proves to be an effective strategy to enhance catalytic performances [54–56]. However, the screening of high-performance heterogeneous electrocatalysts for CO_2 reduction needs to be carried out in a vast parameter space, which is hard to be accomplished by conventional methods. High-throughput methods are well suited to address the challenge and have been developed to screen high-performance CO_2 reduction electrocatalysts.

3. High-Throughput Computational Methods

Generally, high-throughput screening methods can be divided into high-throughput computational methods and high-throughput experimental methods [57,58]. High-throughput computational methods, such as density functional theory (DFT) [59,60] and machine learning, have been widely used for the screening of high-performance CO_2 reduction electrocatalysts [61–63]. DFT is able to calculate the adsorption energy of intermediates on the catalyst surface, thus predicting the catalytic performance [32,64,65]. However, DFT is computationally expensive and requires professional knowledge and specific training. Machine learning can mine the hidden information behind existing data on catalysts and predict the performance of catalysts with different compositions [66]. However, machine learning is hard to uncover the underlying mechanism behind the composition-activity relationships [67]. Therefore, DFT and machine learning are often applied jointly for high-throughput screening by predicting the catalytic activity, identifying the active center, optimizing catalyst composition, and understanding the reaction pathway.

A typical screening process using machine learning includes data collection, data processing, model building, and model optimization, as shown in Figure 2a [68,69]. First, data on the composition, structure, electrochemical property, and catalytic performance of catalyst candidates are collected. Second, the data are processed using feature engineering methods to obtain descriptors, which can be used to build the machine learning model. Then, a machine learning model is established to predict catalytic activity, identify the active center, optimize catalyst composition and understand the reaction pathway [70]. Finally, the model is optimized with experimental data.

The activity of catalysts is usually characterized by adsorption energy and binding energy. Therefore, adsorption energy and binding energy of CO_2 electrocatalytic intermediates are often used to predict the activity of catalysts [71]. For example, DFT and supervised learning are used to obtain the adsorption energies of CO and H at all positions on the surfaces of two types of high-entropy alloys to obtain high-performance alloy catalysts for CO_2 reduction [72]. The spatial maps of CORR activity versus CO_2RR/CORR selectivity for CoCuGaNiZn and AgAuCuPdPt systems are shown in Figure 2b [72].

The type and nature of active sites on the catalysts strongly influence the performance of CO_2 conversion to various products. However, it is still hard to determine the active

sites on the catalysts [73]. Advanced computational methods can address some of the limitations by uncovering the structure-activity relationship. For example, a framework, which uses machine learning to guide DFT calculation and uses active learning for model optimization, is proposed to predict the performance of CO_2 electrocatalytic reduction and has successfully screened 131 surfaces of 34 alloys for CO_2 electrocatalytic reduction [74]. Alternatively, machine learning, multiscale simulation, and quantum mechanics are combined together to predict the surface activity of gold nanoparticles and dealloyed golds and have successfully identified the optimal active sites for CO_2 electrocatalytic reduction, greatly reducing the computational effort [75].

The composition of catalysts could also be optimized by high-throughput computational methods. For example, DFT calculation and active learning are used to predict the adsorption energy of intermediates for CO_2 electrocatalytic reduction to ethylene and systematically adjust the catalyst composition to optimize the performance of Cu-Al alloys and obtain the high-performance catalyst composition [61].

High-throughput computational methods can also predict the free energy of the reaction pathways of CO_2 electrocatalytic reduction [76]. For example, DFT and machine learning are used to predict the activity and reaction pathways of CO_2 reduction by hundreds of transition metal phthalocyanine catalysts [77]. Both DFT and machine learning show similar results for the predicted reaction pathways, and the screening efficiency is improved by 6.87 times, as shown in Figure 2c.

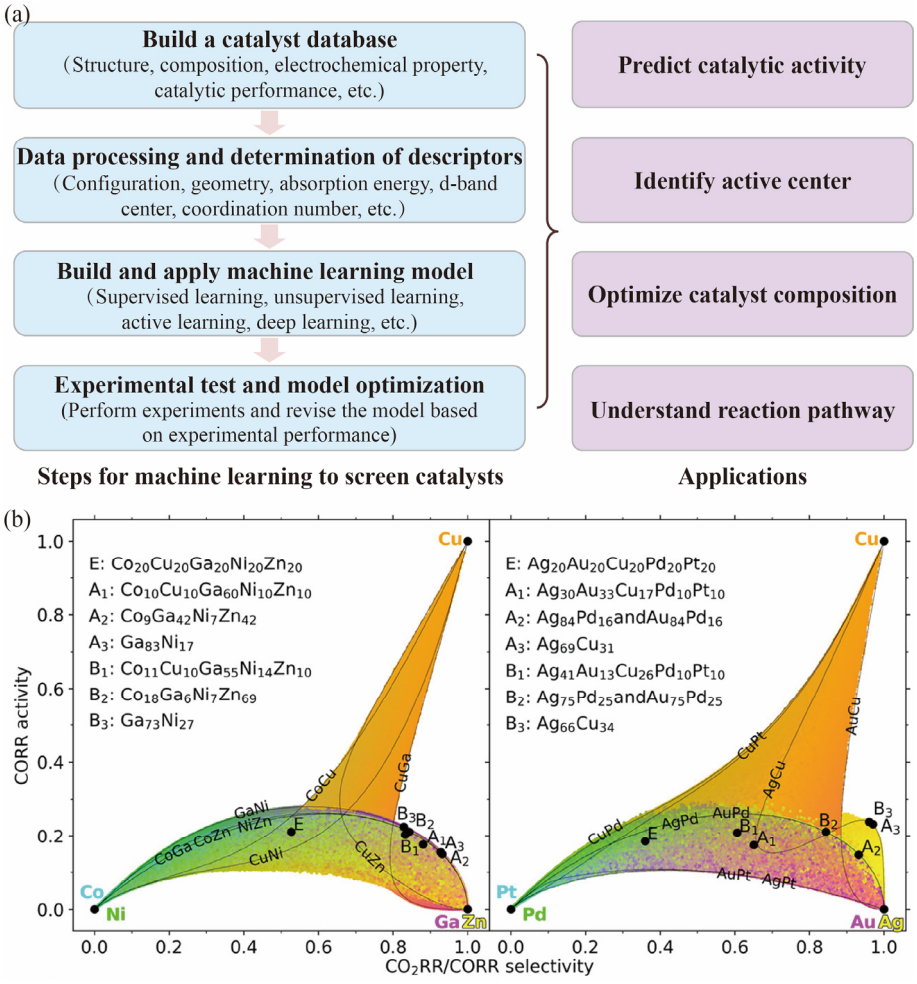

Figure 2. *Cont.*

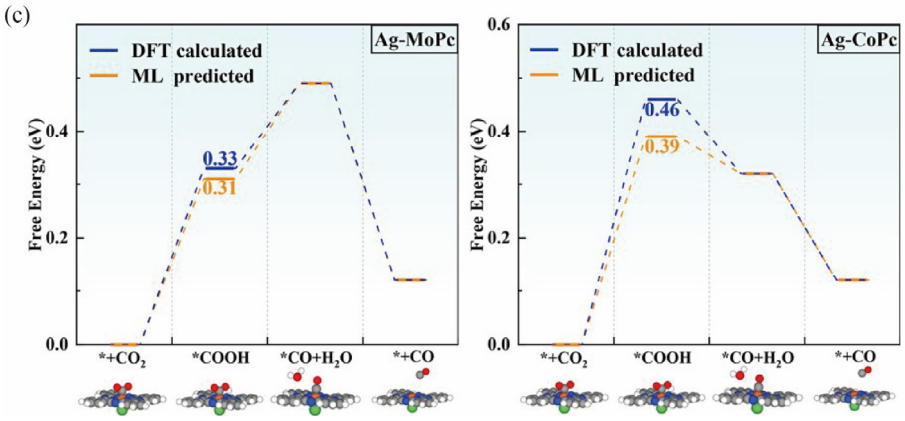

Figure 2. Applications of machine learning in high-throughput screening of high-performance electrocatalysts for CO_2 reduction. (**a**) Steps of machine learning for high-throughput screening. Adapted with permission from Ref. [68]. Copyright 2022, John Wiley and Sons. (**b**) Plots of CORR activity versus CO_2RR/CORR selectivity for CoCuGaNiZn systems (left) and AgAuCuPdPt systems (right) predicted by Gaussian process regression. Reprinted with permission from Ref. [72]. Copyright 2020, American Chemical Society. CORR denotes CO reduction reaction. CO_2RR/CORR selectivity is defined as the probability of surface sites with weaker or the same H adsorption strength as Cu. CORR activity is defined as the ability to reduce CO further, as the joint independent probability of surface sites with weaker or the same H adsorption strength as Cu and stronger or the same CO adsorption strength as Cu. (**c**) ML-predicted and DFT-calculated free energies of different reaction pathways for CO_2RR to CO by Ag-MoPc (left) and Ag-CoPc (right). The * at the upper left of the substance name denotes that the substance is adsorbed on the surface of a catalyst. Reprinted with permission from Ref. [77]. Copyright 2021, American Chemical Society.

High-throughput computational methods, such as DFT and machine learning, have made substantial progress in screening high-performance electrocatalysts for CO_2 reduction. However, predicted results need to be verified by experiments [78]. In return, experimental results will help to revise the computational models for better prediction. Nevertheless, screening high-performance CO_2 electrocatalysts will benefit both the development of machine learning algorithms and the continuous increase of catalyst data.

4. High-Throughput Experimental Methods

The demand for large data by high-throughput computational methods can be solved to a certain extent by high-throughput experimental methods. The steps of a typical experimental process involved in high-throughput screening of high-performance electrocatalysts for CO_2 reduction include: (1) design of experiment, (2) high-throughput synthesis, (3) high-throughput testing, and (4) feedback and optimization, as shown in Figure 3 [57]. The essential of high-throughput experimental approaches to screen out the catalyst with the best performance is the high-throughput synthesis and testing of many catalyst candidates in parallel, which greatly benefit from the development of automation and advanced in situ technology [79–81].

4.1. Experimental Design

The goal of experimental design is to simplify the experimental route to facilitate the high-throughput screening of high-performance catalysts from a large sample reservoir. Determining the potential parameter space and reducing the potential parameter space effectively after each experiment are the two keys of experimental design [57]. Therefore, before performing experiments, collecting parameters as many as possible is necessary to determine the potential parameter space. Then, designing a strategy to explore the potential parameter space and reduce it to a smaller potential parameter space after each experiment is essential.

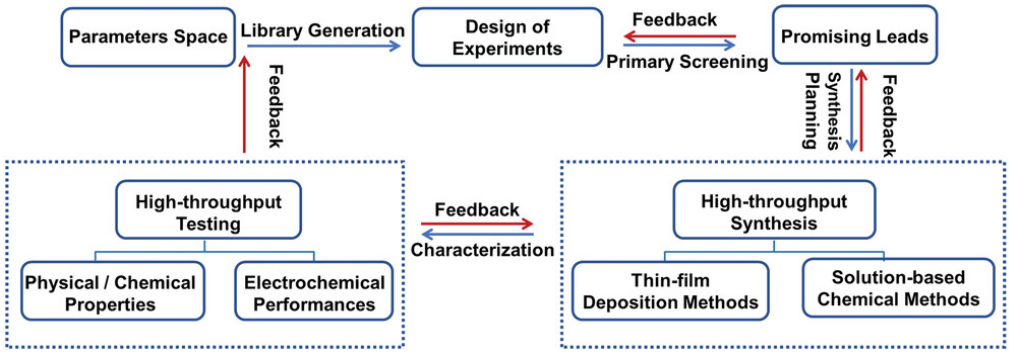

Figure 3. General experimental steps involved in high-throughput screening of high-performance electrocatalysts for CO_2 reduction. Reprinted with permission from Ref. [57]. Copyright 2022, John Wiley and Sons.

For example, an ultrafast multidimensional group testing method is proposed to explore the parameter space of a quaternary catalyst, as shown in Figure 4a [82]. The method divides the parameter space into eight subgroups and distinguishes the high-performance subgroups each time. By repeatedly reducing the size of the parameter space and distinguishing the high-performance subgroups, the method quickly screens out the optimal quaternary catalysts for photocatalytic hydrogen evolution.

Deconvolution is an alternative strategy to effectively reduce the number of tests required to identify high-performance catalysts from mixtures of ligands and metal precursors [83]. For example, a combinatorial strategy utilizing deconvolution is developed to discover high-performance catalysts for the dehydrative Friedel-Crafts reaction, as shown in Figure 4b [84]. The methods include two steps: First, screen one or two reaction parameters in a single block of reactions and identify the best result; Second, perform iterative deconvolution of the precatalysts and ligands using the conditions identified in the first step.

The idea of evolution has also been used to optimize the composition of catalysts. For example, the concept of variation and selection is applied to optimize the composition of catalysts generation by generation, and two excellent catalysts for CO_2 reforming of methane are successfully obtained [85].

4.2. High-Throughput Synthesis

After experimental design, high-throughput synthesis is an indispensable step for high-throughput screening. Catalyst synthesis can be divided into solution-based chemical methods and thin-film deposition methods. Solution-based chemical methods start from catalyst precursors in a solution and prepare catalysts through impregnation, precipitation, drying, grinding, and heat treatment. Flexible control of material compositions and largescale flow synthesis are the two main advantages of solution-based chemical methods. For example, to study the effect of different promoters on the performance of CO_2 hydrogenation, Rh catalysts on the surface of SiO_2 are successfully prepared from impregnated nitric acid solutions with various promoters after drying and heat treatment [86].

Thin-film deposition methods mainly include physical vapor deposition [87] and chemical vapor deposition [88,89] and have the advantages of well controlled thickness, good adhesion with a substrate, and reduced waste. For example, thin-film electrocatalysts of Cu doped with different concentrations of Co are prepared by controlled sputtering deposition, as shown in Figure 5a [29]. The system uses high-purity Ar as sputtering gas, and thin films with different compositions of Cu doped with Co are prepared on Si substrates by adjusting the sputtering power. Thin-film deposition methods could prepare catalysts layer by layer and different layers generally have a distinct boundary. For example, the catalyst for CO_2 electroreduction prepared by electron beam deposition consists of a

50 nm-thick Ti layer deposited on a quartz substrate and a 125 nm-thick $Au_{1-y}Pd_y$ layer deposited on the Ti layer, as shown in Figure 5b [90].

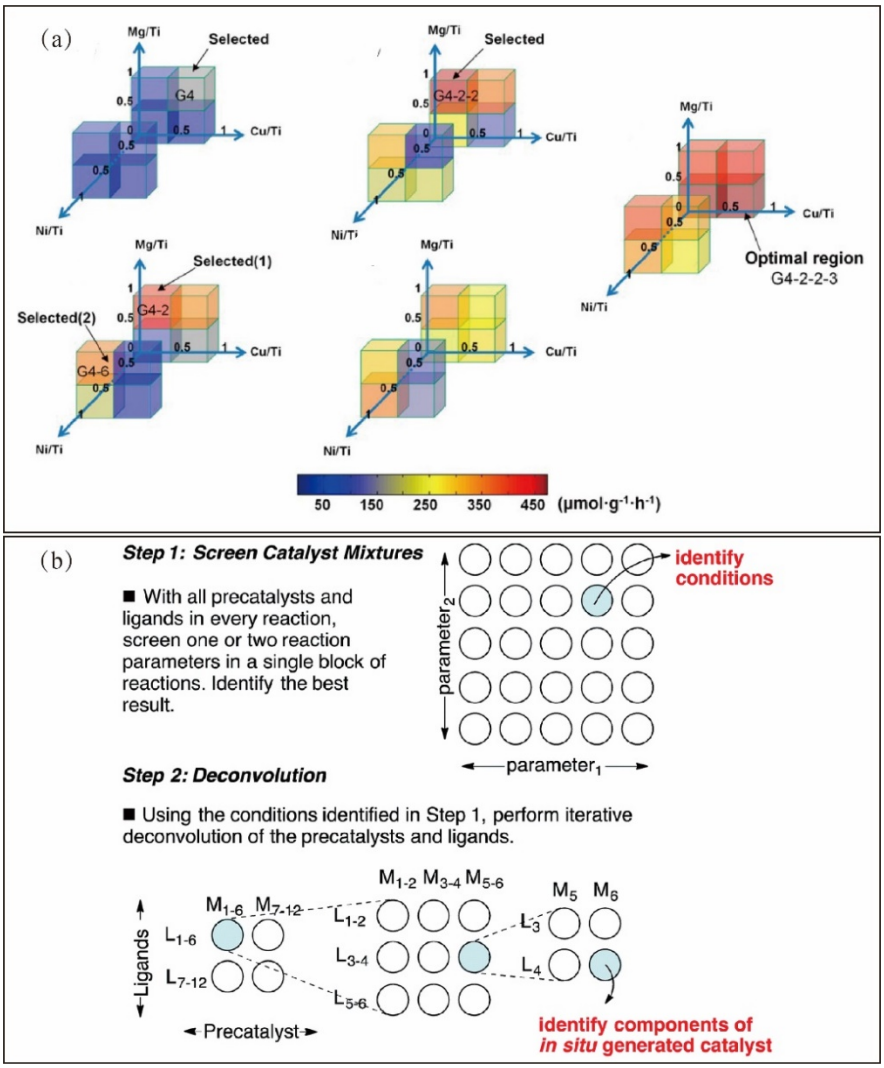

Figure 4. Experimental design for exploring the parameter space of catalysts. (**a**) Identification of the optimal active catalyst for hydrogen production by an ultrafast multidimensional group testing method. Reprinted with permission from Ref. [82]. Copyright 2012, American Chemical Society. (**b**) A combinatorial strategy for identifying lead "hits" in catalyst discovery by deconvolution of complex catalyst mixtures. Reprinted with permission from Ref. [84]. Copyright 2015, The Royal Society of Chemistry.

With the development of advanced technologies, such as automation, high-throughput platforms based on robotics, inkjet printing, and flow reactor have been proposed and applied to the high-throughput synthesis of catalysts [82,85,91]. Robots can perform the precise manipulation of catalyst precursors on microplates, which are either solutions or powders. New pipetting systems and their management software are developed to efficiently manipulate catalyst precursors onto microplates. For example, an open-source management software that can generate efficient pipetting-to-microplate work plans is developed, and its reliable execution is supported by visual guidance, as shown in Figure 5c [92]. The software features a graphical web interface that builds workflows and displays each pipetting step.

Though robots can quickly and accurately dispense precursors for catalyst preparation and a large number of experiments could be realized by robots in parallel, it still takes a long

time to screen multiple variables [83]. In addition, due to the diversity of sample types and the complexity of control programs, widespread applications of robots in high-throughput synthesis are still challenging. To solve the problem, a Bayesian optimization algorithm is applied to drive the robots to realize autonomous operations, as shown in Figure 5d [93]. The Bayesian algorithm autonomously drives the robots to perform 688 experiments in 10 variable spaces in 8 days and find photocatalysts for water splitting with activity six times higher than the original results. Therefore, the Bayesian algorithm avoids the writing of cumbersome control programs and dramatically improves the efficiency of high-throughput synthesis.

Inkjet printing, which is well suited for high-throughput synthesis, only uses a small amount of materials for sample preparation and has a large throughput in mixing different compositions at pre-designed ratios. For example, catalysts with different formulations are prepared for photocatalytic hydrogen evolution using inkjet printing [82]. Generally, the preparation process by inkjet printing includes the configuration of stable colloidal nanoparticle inks, the design of a color management system for mixing, and evaporation-induced self-assembly of nanoparticles, as shown in Figure 5e. During the preparation process, it is essential to develop inks with good dispersity and stability [94]. For example, $AMoO_4$ (A = Ca, Sr, and Ba) inks are prepared by reacting H_2MoO_4 with Ca, Sr, and Ba salts. A series of photocatalysts are prepared by printing different inks together to explore the optimal photocatalysts for the conversion of CO_2 to methanol [95].

Robot and inkjet printing could carry out a large number of reactions in parallel and simultaneously synthesize a variety of catalysts with different compositions. In contrast, microfluidic flow reactors are convenient for controlling synthesis parameters and operating conditions, and synthesized catalysts have better repeatability, uniformity, and catalytic property [96]. Therefore, flow reactors could optimize the quality of catalysts and further improve the performance of catalysts, such as activity and selectivity [97]. For example, CuO-ZnO-ZrO_2 catalysts, which are synthesized by co-precipitation [98] in a microfluidic device, improve the yield of methanol via CO_2 hydrogenation, as shown in Figure 5f [99]. In the microfluidic device, solutions of catalyst precursors are fed into the microfluidic system at a pre-designed ratio and dispersed into 1 mm-diameter droplets. After mixing, catalyst precursors form precipitates within the droplets, and CuO-ZnO-ZrO_2 catalysts with higher specific surface area, better uniformity, and higher activity are made via aging, filtration, drying, and sintering.

4.3. In Situ Characterization

To identify the composition of synthesized catalysts and explore the catalytic process to reveal the underlying mechanism, various characterization techniques are required [100–102]. Typical characterization methods include X-ray diffraction (XRD) and transmission electron microscopy (TEM), which could reveal the crystal lattice of catalysts, mass spectrometry (MS), X-ray energy dispersive spectroscopy (EDS), and X-ray photoelectron spectroscopy (XPS), which could investigate the types and ratios of catalyst compositions, and scanning electron microscopy (SEM), which could analyze the particle morphology and size distribution [103]. Recent applications of various in situ characterization techniques for the structural reconstruction of electrocatalysts, identification of active sites, and recording of intermediates during water electrolysis and CO_2 reduction, are comprehensively summarized, as shown in Figure 6a [104]. For example, the electrochemical reduction of CO_2 by Cu nano catalysts is reconstructed by in situ TEM and operando X-ray absorption spectroscopy investigations [105]. The results suggest that the dissolution and deposition of copper ions is the main reason for the enlargement of catalyst size and the formation of copper oxides plays a vital role in this process.

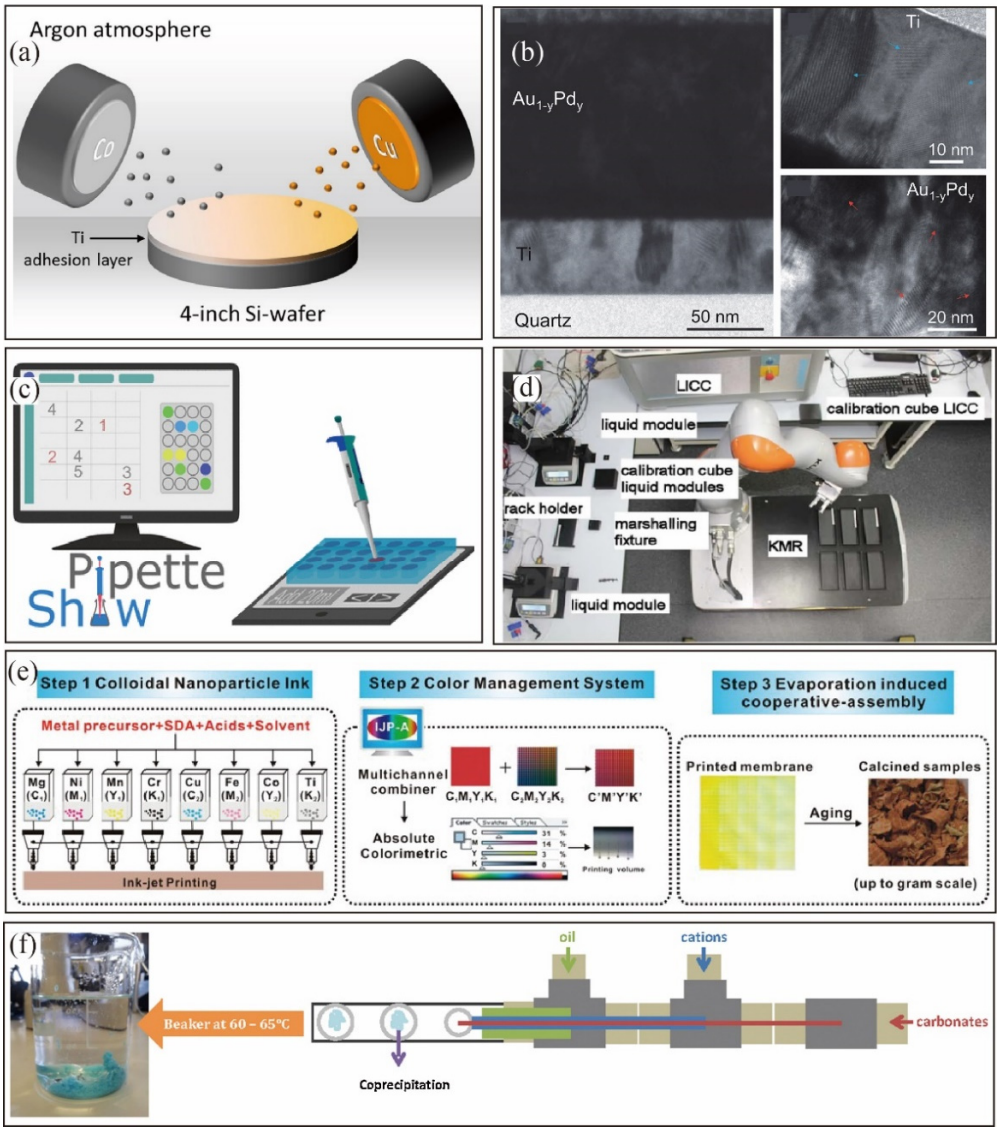

Figure 5. High-throughput synthesis of catalyst candidates. (**a**) Schematic diagram showing the preparation of catalysts by sputtering deposition. Reprinted with permission from Ref. [29]. Copyright 2016, Elsevier. (**b**) Bright-field TEM image of the cross section of a thin multilayer film prepared by electron beam deposition. Reprinted with permission from Ref. [90]. Copyright 2015, The Royal Society of Chemistry. (**c**) An automatic platform that can generate efficient pipetting-to-microplate workplans and support their reliable execution with visual guidance. Reprinted with permission from Ref. [92]. Copyright 2022, American Chemical Society. (**d**) Operations performed autonomously in a combined liquid handling/capping station by mobile robots. Reprinted with permission from Ref. [93]. Copyright 2020, Springer Nature. (**e**) Synthesis of multi-component mesoporous metal oxides using inkjet printing. Reprinted with permission from Ref. [82]. Copyright 2012, American Chemical Society. (**f**) Controlled preparation of catalysts by flow chemistry in microfluidic channels. Reprinted with permission from Ref. [99]. Copyright 2016, Elsevier.

4.4. High-Throughput Testing

Various high-throughput testing techniques, which characterize the catalytic behavior in situ, have been developed to quickly test the performance of catalysts and screen out the catalyst with the best performance. These techniques are mainly based on the characteristics of products, such as the fluorescent or thermal signals measured by a CCD camera [80,106] or the composition and yield of products measured by infrared spectrum [107–110], gas

chromatography and mass spectrometer [36,111,112]. All the methods can quickly measure the compositions and ratios of products in situ and significantly improve the efficiency and accuracy of high-throughput testing.

For example, a fluorescent acid-base indicator is added to the electrolyte. During the electrochemical reduction process of CO_2, platinum catalysts with higher catalytic activity consume more H^+, causing the pH and thus the fluorescent intensity to increase, as shown in Figure 6b [80]. Alternatively, infrared thermal imaging is used to study the catalytic activity of three foam catalysts, e.g., silicon carbide, alumina, and aluminum [113]. When CO_2 is reduced to form methane by the catalysts, heat is released and the catalytic activity is proportional to the amount of released heat, which could qualitatively be characterized by infrared thermal imaging.

High-throughput characterization of catalytic performances by mass spectrometry is mostly realized by designing an automatic stage and exporting the products in situ. For example, a microreactor array with 100 channels is designed for high-throughput screening of alloy film catalysts [114]. After the reaction of gas on the catalyst surface, the product is sent to a mass spectrometer for analysis using a capillary sampler automatically controlled by an x-y positioning stage, as shown in Figure 6c.

Electrochemical performances could also be measured in situ by a mass spectrometer. For example, a scanning flow cell is implemented with an online mass spectrometer to enable rapid in situ detection of reaction products, as shown in Figure 6d [29]. In the experimental setup, a tip, which can direct volatile products of the electrochemical reaction into a mass spectrometer, is incorporated into the flow cell through a PTFE membrane, thus enabling high-throughput in situ analysis.

Alternatively, electrocatalysts are directly coated on the pervaporation membrane to facilitate the volatilization of products into a mass spectrometer and quantify the local performance of the CO_2 electrocatalytic reaction, as shown in Figure 6e [111].

Similarly, a scanning electrochemical flow cell is equipped with an online mass spectrometer to enable quasi-real-time detection of hydrogen, methane, and ethylene, thereby accelerating the screening of electrocatalysts for CO_2 reduction, as shown in Figure 5f [115]. After the electrochemical reaction, the effluent from the flow cell passes through a pervaporation cell to separate gaseous products, which are then pumped to a mass spectrometer for online detection.

After high-throughput testing, the relationship between catalyst composition, and catalytic performance can be investigated and the uncovered relationship could help to reduce the parameter space for the searching of high-performance catalysts. In addition, the obtained experimental results could verify the prediction of high-throughput computing and help to improve the accuracy of high-throughput computing. In return, high-throughput computing will better determine the parameter space and reduce its size, thus improving the efficiency of high-throughput screening.

Despite the important progress made by high-throughput methods in the screening of high-performance CO_2 reduction catalysts, there are still some challenges that need to be addressed. For high-throughput computing, the adaptability, robustness, and explainability of machine learning algorithms and the lack of large data need to be improved, while the high computational cost of DFT and professional knowledge required for DFT make it a challenge for its wide applications. For high-throughput experiments, technologies, such as pipetting robots and inkjet printers, are restricted by factors, such as high cost and limited materials. In addition, the high price of in situ testing equipment and their low versatility also need to be solved. Combining high-throughput computing and high-throughput experiments to better screen high-performance catalysts for CO_2 reduction is of important research value.

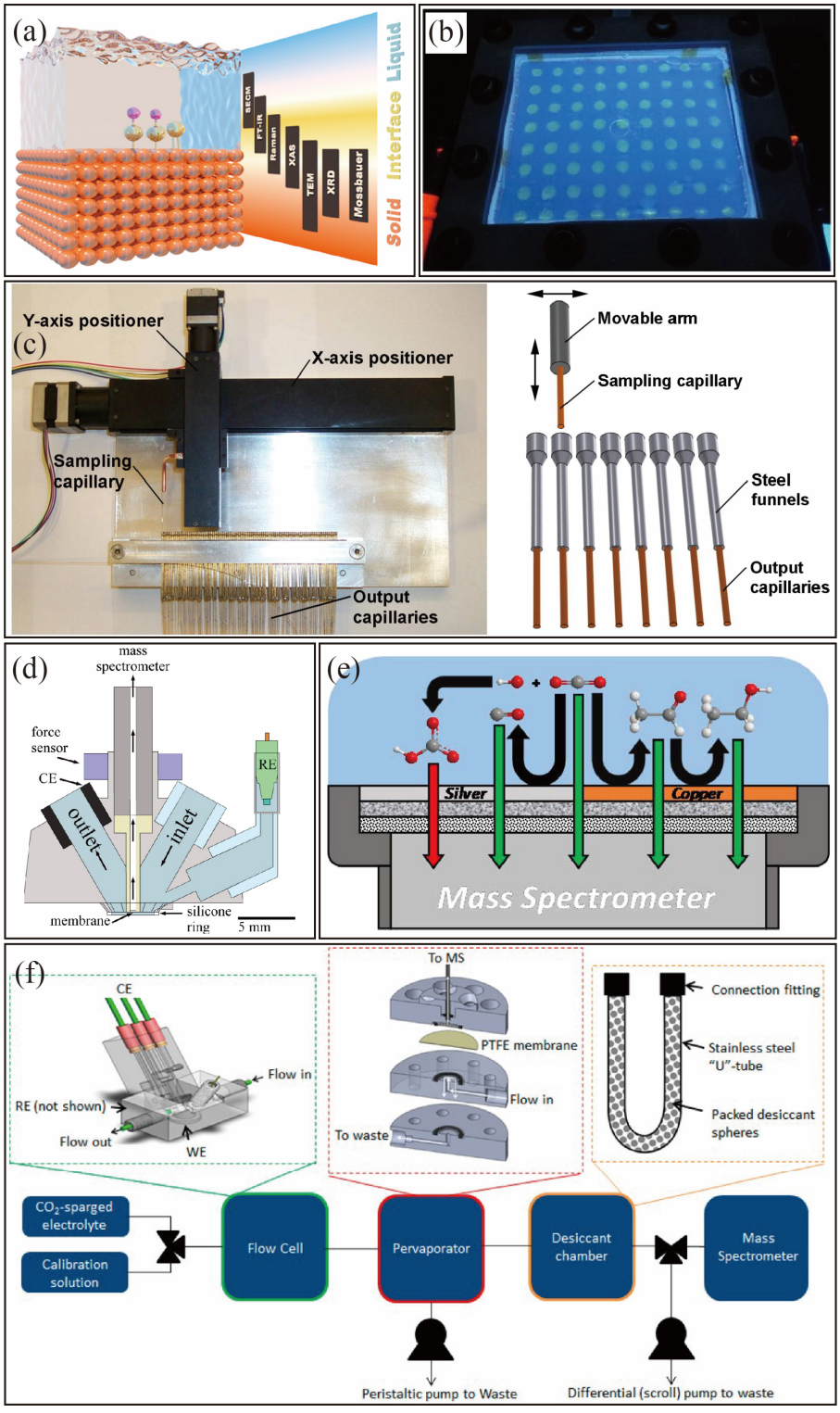

Figure 6. Characterization and high-throughput testing of catalyst candidates. (**a**) In situ characterization methods for solid, interface and liquid catalysts. Reprinted with permission from Ref. [104]. Copyright 2020, American Chemical Society. (**b**) Screening the performance of platinum catalysts by fluorescent intensity. Reprinted with permission from Ref. [80]. Copyright 2021, Springer Nature. (**c**) Automatic, programmable sampling system for multichannel outputs. Reprinted with permission from Ref. [114]. Copyright 2013, Elsevier. (**d**) In situ characterization of the electrochemical performance by mass spectrometry. Reprinted with permission from Ref. [29]. Copyright 2016, Elsevier. (**e**) In situ characterization of the concentration of CO_2 and reaction products near the cathode surface

by mass spectrometry. Reprinted with permission from Ref. [111]. Copyright 2018, American Chemical Society. (**f**) Schematic diagram of an electrochemical flow cell with in situ product detection by mass spectrometry. Reprinted with permission from Ref. [115]. Copyright 2019, American Chemical Society.

5. Conclusions

The conversion and utilization of CO_2 have a dual significance in reducing carbon emissions and solving energy demand. However, CO_2 reduction catalysts with high activity, selectivity, and stability are still lacking. High-throughput screening provides an efficient and low-cost strategy for the searching of high-performance CO_2 reduction catalysts. This review summarizes the research progress on high-throughput screening of high-performance CO_2 reduction catalysts. The catalytic mechanism, influencing factors, and catalyst candidates for CO_2 electrocatalytic reduction are summarized, which provide a reference for understanding the CO_2 electrocatalytic process and selecting catalyst candidates. High-throughput computational methods are introduced with emphasis on the application of density functional theory that investigates the underlying mechanism and machine learning that accelerates the screening efficiency. High-throughput experimental methods include experimental design, high-throughput synthesis, in situ characterization, and high-throughput testing, which improve the experimental efficiency. Promising directions for high-throughput screening of high-performance catalysts include: (1) High-performance multicomponent Cu-based catalysts. Cu is relatively inexpensive but capable of producing different hydrocarbons, while multicomponent Cu-based catalysts could effectively improve the catalytic activity. (2) High-throughput platforms with the combination of high-throughput computational and experimental methods. The large data that machine learning relies on can be obtained by high-throughput experiments. In return, machine learning can effectively reduce the parameter space and provide guidance for high-throughput experiments, thus improving the screening efficiency. (3) In situ high-throughput testing techniques. Current high-throughput platforms are mainly limited by high-throughput screening of catalytic performances. In situ high-throughput testing can quickly obtain experimental data under operating conditions and ensure the efficiency and accuracy of catalyst screening.

Author Contributions: Conceptualization, D.C. and X.G.; methodology, Q.W., M.P., S.Z. and Y.Y.; validation M.P., Y.Y. and D.C.; investigation, Q.W., D.S. and S.Z.; resources, D.C., D.A.W. and X.G.; data curation, S.Z. and D.S.; writing-original draft preparation, M.P. and D.S.; writing-review and editing, Q.W. and D.C.; supervision, D.C. and X.G.; project administration, D.C., D.A.W. and X.G.; funding acquisition, D.C. All authors have read and agreed to the published version of the manuscript.

Funding: This research was funded by Zhejiang Provincial Natural Science Foundation of China (Grant No. Y20B060027), Zhejiang University Global Partnership Fund, National Natural Science Foundation of China (Grant No. 21878258), and National Key Research and Development Program of China (YS2021YFC3000089). This work is also supported by the National Science Foundation (DMR1310266) and the Harvard Materials Research Science and Engineering Center (DMR-2011754).

Institutional Review Board Statement: Not applicable.

Informed Consent Statement: Not applicable.

Data Availability Statement: Not applicable.

Conflicts of Interest: The authors declare no conflict of interest.

References

1. Seh, Z.W.; Kibsgaard, J.; Dickens, C.F.; Chorkendorff, I.; Nørskov, J.K.; Jaramillo, T.F. Combining theory and experiment in electrocatalysis: Insights into materials design. *Science* **2017**, *355*, eaad4998. [CrossRef] [PubMed]
2. Peter, S.C. Reduction of CO_2 to chemicals and fuels: A solution to global warming and energy crisis. *ACS Energy Lett.* **2018**, *3*, 1557–1561. [CrossRef]

3. Zhong, H.; Ghorbani-Asl, M.; Ly, K.H.; Zhang, J.; Ge, J.; Wang, M.; Liao, Z.; Makarov, D.; Zschech, E.; Brunner, E. Synergistic electroreduction of carbon dioxide to carbon monoxide on bimetallic layered conjugated metal-organic frameworks. *Nat. Commun.* **2020**, *11*, 1–10.
4. Kattel, S.; Ramírez, P.J.; Chen, J.G.; Rodriguez, J.A.; Liu, P. Active sites for CO_2 hydrogenation to methanol on Cu/ZnO catalysts. *Science* **2017**, *355*, 1296–1299. [CrossRef]
5. Arandiyan, H.; Kani, K.; Wang, Y.; Jiang, B.; Kim, J.; Yoshino, M.; Rezaei, M.; Rowan, A.E.; Dai, H.; Yamauchi, Y. Highly selective reduction of carbon dioxide to methane on novel mesoporous Rh catalysts. *ACS Appl. Mater. Interfaces* **2018**, *10*, 24963–24968. [CrossRef]
6. Phillips, K.R.; Katayama, Y.; Hwang, J.; Shao-Horn, Y. Sulfide-Derived Copper for Electrochemical Conversion of CO_2 to Formic Acid. *J. Phys. Chem. Lett.* **2018**, *9*, 4407–4412. [CrossRef] [PubMed]
7. Costa, R.S.; Aranha, B.S.; Ghosh, A.; Lobo, A.O.; da Silva, E.T.; Alves, D.C.; Viana, B.C. Production of oxalic acid by electrochemical reduction of CO_2 using silver-carbon material from babassu coconut mesocarp. *J. Phys. Chem. Solids* **2020**, *147*, 109678. [CrossRef]
8. Chan, F.L.; Altinkaya, G.; Fung, N.; Tanksale, A. Low temperature hydrogenation of carbon dioxide into formaldehyde in liquid media. *Catal. Today* **2018**, *309*, 242–247. [CrossRef]
9. Kim, S.; Yang, Y.; Lippi, R.; Choi, H.; Kim, S.; Chun, D.; Im, H.; Lee, S.; Yoo, J. Low-Rank Coal Supported Ni Catalysts for CO_2 Methanation. *Energies* **2021**, *14*, 2040. [CrossRef]
10. Nair, M.M.; Abanades, S.p. Tailoring hybrid nonstoichiometric ceria redox cycle for combined solar methane reforming and thermochemical conversion of H_2O/CO_2. *Energy Fuels* **2016**, *30*, 6050–6058. [CrossRef]
11. Hare, B.J.; Maiti, D.; Ramani, S.; Ramos, A.E.; Bhethanabotla, V.R.; Kuhn, J.N. Thermochemical conversion of carbon dioxide by reverse water-gas shift chemical looping using supported perovskite oxides. *Catal. Today* **2019**, *323*, 225–232. [CrossRef]
12. Feng, K.; Wang, Y.; Guo, M.; Zhang, J.; Li, Z.; Deng, T.; Zhang, Z.; Yan, B. In-situ/operando techniques to identify active sites for thermochemical conversion of CO_2 over heterogeneous catalysts. *J. Energy Chem.* **2021**, *62*, 153–171. [CrossRef]
13. Suvarna, M.; Araújo, T.P.; Pérez-Ramírez, J. A generalized machine learning framework to predict the space-time yield of methanol from thermocatalytic CO_2 hydrogenation. *Appl. Catal. B* **2022**, 121530. [CrossRef]
14. Huang, H.; Lin, J.; Zhu, G.; Weng, Y.; Wang, X.; Fu, X.; Long, J. A long-lived mononuclear cyclopentadienyl ruthenium complex grafted onto anatase TiO_2 for efficient CO_2 photoreduction. *Angew. Chem. Int. Ed.* **2016**, *55*, 8314–8318. [CrossRef] [PubMed]
15. Chai, Y.; Li, L.; Shen, J.; Zhang, Y.; Liang, J. $Zn_2Sn_xTi_{1-x}O_4$ Continuous Solid-Solution Photocatalyst for Efficient Photocatalytic CO_2 Conversion into Solar Fuels. *ACS Appl. Energy Mater.* **2022**, *5*, 3748–3756. [CrossRef]
16. Cheng, S.; Sun, Z.; Lim, K.H.; Gani, T.Z.H.; Zhang, T.; Wang, Y.; Yin, H.; Liu, K.; Guo, H.; Du, T. Emerging Strategies for CO_2 Photoreduction to CH_4: From Experimental to Data-Driven Design. *Adv. Energy Mater.* **2022**, *12*, 2200389. [CrossRef]
17. Yang, G.; Qiu, P.; Xiong, J.; Zhu, X.; Cheng, G. Facilely anchoring Cu_2O nanoparticles on mesoporous TiO_2 nanorods for enhanced photocatalytic CO_2 reduction through efficient charge transfer. *Chin. Chem. Lett.* **2022**, *33*, 3709–3712. [CrossRef]
18. Sen, S.; Liu, D.; Palmore, G.T.R. Electrochemical reduction of CO_2 at copper nanofoams. *ACS Catal.* **2014**, *4*, 3091–3095. [CrossRef]
19. Xie, H.; Wang, T.; Liang, J.; Li, Q.; Sun, S. Cu-based nanocatalysts for electrochemical reduction of CO_2. *Nano Today* **2018**, *21*, 41–54. [CrossRef]
20. Jiang, K.; Huang, Y.; Zeng, G.; Toma, F.M.; Goddard, W.A., III; Bell, A.T. Effects of surface roughness on the electrochemical reduction of CO_2 over Cu. *ACS Energy Lett.* **2020**, *5*, 1206–1214. [CrossRef]
21. Masana, J.J.; Peng, B.; Shuai, Z.; Qiu, M.; Yu, Y. Influence of Halide Ions on Electrochemical Reduction of Carbon dioxide over Copper Surface. *J. Mater. Chem. A* **2022**, *10*, 1086. [CrossRef]
22. Liu, C.; Colón, B.C.; Ziesack, M.; Silver, P.A.; Nocera, D.G. Water splitting–biosynthetic system with CO_2 reduction efficiencies exceeding photosynthesis. *Science* **2016**, *352*, 1210–1213. [CrossRef] [PubMed]
23. Hu, B.; Harris, D.F.; Dean, D.R.; Liu, T.L.; Yang, Z.-Y.; Seefeldt, L.C. Electrocatalytic CO_2 reduction catalyzed by nitrogenase MoFe and FeFe proteins. *Bioelectrochemistry* **2018**, *120*, 104–109. [CrossRef]
24. Shafaat, H.S.; Yang, J.Y. Uniting biological and chemical strategies for selective CO_2 reduction. *Nat. Catal.* **2021**, *4*, 928–933. [CrossRef]
25. Lopes, E.J.; Ribeiro, A.P.; Martins, L.M. New trends in the conversion of CO_2 to cyclic carbonates. *Catalysts* **2020**, *10*, 479. [CrossRef]
26. Schneider, J.; Jia, H.; Muckerman, J.T.; Fujita, E. Thermodynamics and kinetics of CO_2, CO, and H^+ binding to the metal centre of CO_2 reduction catalysts. *Chem. Soc. Rev.* **2012**, *41*, 2036–2051. [CrossRef] [PubMed]
27. Gong, L.; Zhang, D.; Lin, C.Y.; Zhu, Y.; Shen, Y.; Zhang, J.; Han, X.; Zhang, L.; Xia, Z. Catalytic mechanisms and design principles for single-atom catalysts in highly efficient CO_2 conversion. *Adv. Energy Mater.* **2019**, *9*, 1902625. [CrossRef]
28. Zhang, X.; Guo, S.-X.; Gandionco, K.A.; Bond, A.M.; Zhang, J. Electrocatalytic carbon dioxide reduction: From fundamental principles to catalyst design. *Mater. Today* **2020**, *7*, 100074. [CrossRef]
29. Grote, J.-P.; Zeradjanin, A.R.; Cherevko, S.; Savan, A.; Breitbach, B.; Ludwig, A.; Mayrhofer, K.J. Screening of material libraries for electrochemical CO_2 reduction catalysts—Improving selectivity of Cu by mixing with Co. *J. Catal.* **2016**, *343*, 248–256. [CrossRef]
30. Li, W.; Nie, X.; Jiang, X.; Zhang, A.; Ding, F.; Liu, M.; Liu, Z.; Guo, X.; Song, C. ZrO_2 support imparts superior activity and stability of Co catalysts for CO_2 methanation. *Appl. Catal. B.* **2018**, *220*, 397–408. [CrossRef]
31. Karmodak, N.; Vijay, S.; Kastlunger, G.; Chan, K. Computational Screening of Single and Di-Atom Catalysts for Electrochemical CO_2 Reduction. *ACS Catal.* **2022**, *12*, 4818–4824. [CrossRef]

32. Liu, K.; Wang, J.; Shi, M.; Yan, J.; Jiang, Q. Simultaneous achieving of high faradaic efficiency and CO partial current density for CO_2 reduction via robust, noble-metal-free Zn nanosheets with favorable adsorption energy. *Adv. Energy Mater.* **2019**, *9*, 1900276. [CrossRef]
33. Mayer, F.D.; Hosseini-Benhangi, P.; Sánchez-Sánchez, C.M.; Asselin, E.; Gyenge, E.L. Scanning electrochemical microscopy screening of CO_2 electroreduction activities and product selectivities of catalyst arrays. *Commun. Chem.* **2020**, *3*, 1–9. [CrossRef]
34. De Gregorio, G.L.; Burdyny, T.; Loiudice, A.; Iyengar, P.; Smith, W.A.; Buonsanti, R. Facet-dependent selectivity of Cu catalysts in electrochemical CO_2 reduction at commercially viable current densities. *ACS Catal.* **2020**, *10*, 4854–4862. [CrossRef]
35. Nellaiappan, S.; Katiyar, N.K.; Kumar, R.; Parui, A.; Malviya, K.D.; Pradeep, K.; Singh, A.K.; Sharma, S.; Tiwary, C.S.; Biswas, K. High-entropy alloys as catalysts for the CO_2 and CO reduction reactions: Experimental realization. *ACS Catal.* **2020**, *10*, 3658–3663. [CrossRef]
36. Batchelor, T.A.; Löffler, T.; Xiao, B.; Krysiak, O.A.; Strotkötter, V.; Pedersen, J.K.; Clausen, C.M.; Savan, A.; Li, Y.; Schuhmann, W. Complex-Solid-Solution Electrocatalyst Discovery by Computational Prediction and High-Throughput Experimentation. *Angew. Chem. Int. Ed.* **2021**, *60*, 6932–6937. [CrossRef] [PubMed]
37. Qiao, J.; Liu, Y.; Hong, F.; Zhang, J. A review of catalysts for the electroreduction of carbon dioxide to produce low-carbon fuels. *Chem. Soc. Rev.* **2014**, *43*, 631–675. [CrossRef] [PubMed]
38. Kibria, M.G.; Edwards, J.P.; Gabardo, C.M.; Dinh, C.T.; Seifitokaldani, A.; Sinton, D.; Sargent, E.H. Electrochemical CO_2 reduction into chemical feedstocks: From mechanistic electrocatalysis models to system design. *Adv. Mater.* **2019**, *31*, 1807166. [CrossRef]
39. Zhang, L.; Zhao, Z.J.; Gong, J. Nanostructured materials for heterogeneous electrocatalytic CO_2 reduction and their related reaction mechanisms. *Angew. Chem. Int. Ed.* **2017**, *56*, 11326–11353. [CrossRef]
40. Zheng, Y.; Vasileff, A.; Zhou, X.; Jiao, Y.; Jaroniec, M.; Qiao, S.-Z. Understanding the roadmap for electrochemical reduction of CO_2 to multi-carbon oxygenates and hydrocarbons on copper-based catalysts. *J. Am. Chem. Soc.* **2019**, *141*, 7646–7659. [CrossRef]
41. Handoko, A.D.; Chen, H.; Lum, Y.; Zhang, Q.; Anasori, B.; Seh, Z.W. Two-dimensional titanium and molybdenum carbide MXenes as electrocatalysts for CO_2 reduction. *IScience* **2020**, *23*, 101181. [CrossRef] [PubMed]
42. Hooe, S.L.; Dressel, J.M.; Dickie, D.A.; Machan, C.W. Highly efficient electrocatalytic reduction of CO_2 to CO by a molecular chromium complex. *ACS Catal.* **2019**, *10*, 1146–1151. [CrossRef]
43. He, J.; Dettelbach, K.E.; Huang, A.; Berlinguette, C.P. Brass and bronze as effective CO_2 reduction electrocatalysts. *Angew. Chem. Int. Ed.* **2017**, *129*, 16806–16809. [CrossRef]
44. Li, Z.; He, D.; Yan, X.; Dai, S.; Younan, S.; Ke, Z.; Pan, X.; Xiao, X.; Wu, H.; Gu, J. Size-dependent nickel-based electrocatalysts for selective CO_2 reduction. *Angew. Chem. Int. Ed.* **2020**, *132*, 18731–18736. [CrossRef]
45. Umeda, M.; Niitsuma, Y.; Horikawa, T.; Matsuda, S.; Osawa, M. Electrochemical reduction of CO_2 to methane on platinum catalysts without overpotentials: Strategies for improving conversion efficiency. *ACS Appl. Energy Mater.* **2019**, *3*, 1119–1127. [CrossRef]
46. Ma, M.; Liu, K.; Shen, J.; Kas, R.; Smith, W.A. In Situ fabrication and reactivation of highly selective and stable Ag catalysts for electrochemical CO_2 conversion. *ACS Energy Lett.* **2018**, *3*, 1301–1306. [CrossRef]
47. Zhang, Y.-J.; Sethuraman, V.; Michalsky, R.; Peterson, A.A. Competition between CO_2 reduction and H_2 evolution on transition-metal electrocatalysts. *ACS Catal.* **2014**, *4*, 3742–3748. [CrossRef]
48. Wang, Z.; She, X.; Yu, Q.; Zhu, X.; Li, H.; Xu, H. Minireview on the Commonly Applied Copper-Based Electrocatalysts for Electrochemical CO_2 Reduction. *Energy Fuels* **2021**, *35*, 8585–8601. [CrossRef]
49. Kuhl, K.P.; Cave, E.R.; Abram, D.N.; Jaramillo, T.F. New insights into the electrochemical reduction of carbon dioxide on metallic copper surfaces. *Energy Environ. Sci.* **2012**, *5*, 7050–7059. [CrossRef]
50. Schouten, K.J.P.; Gallent, E.P.; Koper, M.T. The influence of pH on the reduction of CO and CO_2 to hydrocarbons on copper electrodes. *J. Electroanal. Chem.* **2014**, *716*, 53–57. [CrossRef]
51. Wang, L.; Nitopi, S.A.; Bertheussen, E.; Orazov, M.; Morales-Guio, C.G.; Liu, X.; Higgins, D.C.; Chan, K.; Nørskov, J.K.; Hahn, C. Electrochemical carbon monoxide reduction on polycrystalline copper: Effects of potential, pressure, and pH on selectivity toward multicarbon and oxygenated products. *ACS Catal.* **2018**, *8*, 7445–7454. [CrossRef]
52. Wu, J.; Sharifi, T.; Gao, Y.; Zhang, T.; Ajayan, P.M. Emerging carbon-based heterogeneous catalysts for electrochemical reduction of carbon dioxide into value-added chemicals. *Adv. Mater.* **2019**, *31*, 1804257. [CrossRef] [PubMed]
53. Zhao, K.; Quan, X. Carbon-based materials for electrochemical reduction of CO_2 to C_{2+} oxygenates: Recent progress and remaining challenges. *ACS Catal.* **2021**, *11*, 2076–2097. [CrossRef]
54. Martínez-Hincapié, R.; Čolić, V. Electrocatalysts for the Oxygen Reduction Reaction: From Bimetallic Platinum Alloys to Complex Solid Solutions. *ChemEng.* **2022**, *6*, 19. [CrossRef]
55. Chen, S.; Liu, T.; Olanrele, S.O.; Lian, Z.; Si, C.; Chen, Z.; Li, B. Boosting electrocatalytic activity for CO_2 reduction on nitrogen-doped carbon catalysts by co-doping with phosphorus. *J. Energy Chem.* **2021**, *54*, 143–150. [CrossRef]
56. Löffler, T.; Ludwig, A.; Rossmeisl, J.; Schuhmann, W. What Makes High-Entropy Alloys Exceptional Electrocatalysts? *Angew. Chem. Int. Ed.* **2021**, *60*, 26894–26903. [CrossRef]
57. Liu, X.; Liu, B.; Ding, J.; Deng, Y.; Han, X.; Zhong, C.; Hu, W. Building a Library for Catalysts Research Using High-Throughput Approaches. *Adv. Funct. Mater.* **2022**, 2107862. [CrossRef]
58. Steinmann, S.N.; Hermawan, A.; Jassar, M.B.; Seh, Z.W. Autonomous high-throughput computations in catalysis. *Chem Catal.* **2022**, *2*, 917–1240. [CrossRef]

59. Qin, X.; Zhu, S.; Xiao, F.; Zhang, L.; Shao, M. Active sites on heterogeneous single-iron-atom electrocatalysts in CO_2 reduction reaction. *ACS Energy Lett.* **2019**, *4*, 1778–1783. [CrossRef]
60. Tian, D.; Denny, S.R.; Li, K.; Wang, H.; Kattel, S.; Chen, J.G. Density functional theory studies of transition metal carbides and nitrides as electrocatalysts. *Chem. Soc. Rev.* **2021**, *50*, 12338. [CrossRef]
61. Zhong, M.; Tran, K.; Min, Y.; Wang, C.; Wang, Z.; Dinh, C.-T.; De Luna, P.; Yu, Z.; Rasouli, A.S.; Brodersen, P. Accelerated discovery of CO_2 electrocatalysts using active machine learning. *Nature.* **2020**, *581*, 178–183. [CrossRef] [PubMed]
62. Yang, Z.; Gao, W.; Jiang, Q. A machine learning scheme for the catalytic activity of alloys with intrinsic descriptors. *J. Mater. Chem. A.* **2020**, *8*, 17507–17515. [CrossRef]
63. Ting, K.W.; Kamakura, H.; Poly, S.S.; Takao, M.; Siddiki, S.H.; Maeno, Z.; Matsushita, K.; Shimizu, K.-i.; Toyao, T. Catalytic Methylation of m-Xylene, Toluene, and Benzene Using CO_2 and H_2 over TiO_2-Supported Re and Zeolite Catalysts: Machine-Learning-Assisted Catalyst Optimization. *ACS Catal.* **2021**, *11*, 5829–5838. [CrossRef]
64. Zhi, X.; Jiao, Y.; Zheng, Y.; Qiao, S.Z. Impact of interfacial electron transfer on electrochemical CO_2 reduction on graphitic carbon nitride/doped graphene. *Small* **2019**, *15*, 1804224. [CrossRef] [PubMed]
65. Zhang, N.; Zhang, X.; Kang, Y.; Ye, C.; Jin, R.; Yan, H.; Lin, R.; Yang, J.; Xu, Q.; Wang, Y. A supported Pd_2 dual-atom site catalyst for efficient electrochemical CO_2 reduction. *Angew. Chem. Int. Ed.* **2021**, *133*, 13500–13505. [CrossRef]
66. McCullough, K.; Williams, T.; Mingle, K.; Jamshidi, P.; Lauterbach, J. High-throughput experimentation meets artificial intelligence: A new pathway to catalyst discovery. *Phys. Chem. Chem. Phys.* **2020**, *22*, 11174–11196. [CrossRef]
67. Ribeiro, M.T.; Singh, S.; Guestrin, C. "Why should I trust you"? Explaining the predictions of any classifier. In Proceedings of the 22nd ACM SIGKDD International Conference on Knowledge Discovery and Data Mining, San Francisco, CA, USA, 13–17 August 2016; pp. 1135–1144.
68. Sun, Z.; Yin, H.; Liu, K.; Cheng, S.; Li, G.K.; Kawi, S.; Zhao, H.; Jia, G.; Yin, Z. Machine learning accelerated calculation and design of electrocatalysts for CO_2 reduction. *SmartMat* **2022**, *3*, 68–83. [CrossRef]
69. Dong, Y.; Zhang, Y.; Ran, M.; Zhang, X.; Liu, S.; Yang, Y.; Hu, W.; Zheng, C.; Gao, X. Accelerated identification of high-performance catalysts for low-temperature NH_3-SCR by machine learning. *J. Mater. Chem. A* **2021**, *9*, 23850–23859. [CrossRef]
70. Zhang, N.; Yang, B.; Liu, K.; Li, H.; Chen, G.; Qiu, X.; Li, W.; Hu, J.; Fu, J.; Jiang, Y. Machine Learning in Screening High Performance Electrocatalysts for CO_2 Reduction. *Small Methods* **2021**, *5*, 2100987. [CrossRef]
71. Roy, D.; Mandal, S.C.; Pathak, B. Machine Learning-Driven High-Throughput Screening of Alloy-Based Catalysts for Selective CO_2 Hydrogenation to Methanol. *ACS Appl. Mater. Interfaces* **2021**, *13*, 56151–56163. [CrossRef]
72. Pedersen, J.K.; Batchelor, T.A.; Bagger, A.; Rossmeisl, J. High-entropy alloys as catalysts for the CO_2 and CO reduction reactions. *ACS Catal.* **2020**, *10*, 2169–2176. [CrossRef]
73. Daiyan, R.; Saputera, W.H.; Masood, H.; Leverett, J.; Lu, X.; Amal, R. A Disquisition on the Active Sites of Heterogeneous Catalysts for Electrochemical Reduction of CO_2 to Value-Added Chemicals and Fuel. *Adv. Energy Mater.* **2020**, *10*, 1902106. [CrossRef]
74. Tran, K.; Ulissi, Z.W. Active learning across intermetallics to guide discovery of electrocatalysts for CO_2 reduction and H_2 evolution. *Nat. Catal.* **2018**, *1*, 696–703. [CrossRef]
75. Chen, Y.; Huang, Y.; Cheng, T.; Goddard, W.A., III. Identifying active sites for CO_2 reduction on dealloyed gold surfaces by combining machine learning with multiscale simulations. *J. Am. Chem. Soc.* **2019**, *141*, 11651–11657. [CrossRef] [PubMed]
76. He, C.; Yang, H.; Fu, X.; Cheng, X.; Guo, J.; Fu, L. A DFT study of two-dimensional P_2Si monolayer modified by single transition metal (Sc-Cu) atoms for efficient electrocatalytic CO_2 reduction. *Chin. Chem. Lett.* **2022**. [CrossRef]
77. Wan, X.; Zhang, Z.; Niu, H.; Yin, Y.; Kuai, C.; Wang, J.; Shao, C.; Guo, Y. Machine-Learning-Accelerated Catalytic Activity Predictions of Transition Metal Phthalocyanine Dual-Metal-Site Catalysts for CO_2 Reduction. *J. Phys. Chem. Lett.* **2021**, *12*, 6111–6118. [CrossRef] [PubMed]
78. Liu, J.; Luo, W.; Wang, L.; Zhang, J.; Fu, X.Z.; Luo, J.L. Toward Excellence of Electrocatalyst Design by Emerging Descriptor-Oriented Machine Learning. *Adv. Funct. Mater.* **2022**, *32*, 2110748. [CrossRef]
79. Lai, Y.; Jones, R.J.; Wang, Y.; Zhou, L.; Richter, M.H.; Gregoire, J. The sensitivity of Cu for electrochemical carbon dioxide reduction to hydrocarbons as revealed by high throughput experiments. *J. Mater. Chem. A.* **2019**, *7*, 26785–26790. [CrossRef]
80. Hitt, J.L.; Li, Y.C.; Tao, S.; Yan, Z.; Gao, Y.; Billinge, S.J.; Mallouk, T.E. A high throughput optical method for studying compositional effects in electrocatalysts for CO_2 reduction. *Nat. Commun.* **2021**, *12*, 1–10.
81. Lai, Y.; Watkins, N.B.; Rosas-Hernández, A.; Thevenon, A.; Heim, G.P.; Zhou, L.; Wu, Y.; Peters, J.C.; Gregoire, J.M.; Agapie, T. Breaking Scaling Relationships in CO_2 Reduction on Copper Alloys with Organic Additives. *ACS Cent. Sci.* **2021**, *7*, 1756–1762. [CrossRef]
82. Liu, X.; Shen, Y.; Yang, R.; Zou, S.; Ji, X.; Shi, L.; Zhang, Y.; Liu, D.; Xiao, L.; Zheng, X. Inkjet printing assisted synthesis of multicomponent mesoporous metal oxides for ultrafast catalyst exploration. *Nano Lett.* **2012**, *12*, 5733–5739. [CrossRef] [PubMed]
83. Renom-Carrasco, M.; Lefort, L. Ligand libraries for high throughput screening of homogeneous catalysts. *Chem. Soc. Rev.* **2018**, *47*, 5038–5060. [CrossRef] [PubMed]
84. Wolf, E.; Richmond, E.; Moran, J. Identifying lead hits in catalyst discovery by screening and deconvoluting complex mixtures of catalyst components. *Chem. Sci.* **2015**, *6*, 2501–2505. [CrossRef] [PubMed]
85. Kim, D.K.; Maier, W.F. Combinatorial discovery of new autoreduction catalysts for the CO_2 reforming of methane. *J. Catal.* **2006**, *238*, 142–152. [CrossRef]

86. Goryachev, A.; Pustovarenko, A.; Shterk, G.; Alhajri, N.S.; Jamal, A.; Albuali, M.; van Koppen, L.; Khan, I.S.; Russkikh, A.; Ramirez, A. A Multi-Parametric Catalyst Screening for CO_2 Hydrogenation to Ethanol. *ChemCatChem* **2021**, *13*, 3324–3332. [CrossRef]
87. Jeng, E.; Qi, Z.; Kashi, A.R.; Hunegnaw, S.; Huo, Z.; Miller, J.S.; Bayu Aji, L.B.; Ko, B.H.; Shin, H.; Ma, S. Scalable gas diffusion electrode fabrication for electrochemical CO_2 reduction using physical vapor deposition methods. *ACS Appl. Mater. Interfaces* **2022**, *14*, 7731–7740. [CrossRef]
88. Kortlever, R.; Peters, I.; Balemans, C.; Kas, R.; Kwon, Y.; Mul, G.; Koper, M. Palladium–gold catalyst for the electrochemical reduction of CO_2 to C_1–C_5 hydrocarbons. *Chem. Commun.* **2016**, *52*, 10229–10232. [CrossRef]
89. Zanellato, G.; Schiavi, P.G.; Zanoni, R.; Rubino, A.; Altimari, P.; Pagnanelli, F. Electrodeposited Copper Nanocatalysts for CO_2 Electroreduction: Effect of Electrodeposition Conditions on Catalysts' Morphology and Selectivity. *Energies* **2021**, *14*, 5012. [CrossRef]
90. Hahn, C.; Abram, D.N.; Hansen, H.A.; Hatsukade, T.; Jackson, A.; Johnson, N.C.; Hellstern, T.R.; Kuhl, K.P.; Cave, E.R.; Feaster, J.T. Synthesis of thin film AuPd alloys and their investigation for electrocatalytic CO_2 reduction. *J. Mater. Chem. A* **2015**, *3*, 20185–20194. [CrossRef]
91. Zhang, M.; Lee, J.; Wang, L.; Duan, Q.; Zhang, J.; Qi, H. A Novel High-Throughput Screening of Multicomponent Photocatalysts for Decomposition of Organic Pollutants Based on Fluorescence Imaging. *ChemCatChem* **2015**, *7*, 3978–3984. [CrossRef]
92. Falk, J.; Mendler, M.; Kabisch, J. Pipette Show: An Open Source Web Application to Support Pipetting into Microplates. *ACS Synth. Biol.* **2022**, *11*, 996–999. [CrossRef] [PubMed]
93. Burger, B.; Maffettone, P.M.; Gusev, V.V.; Aitchison, C.M.; Bai, Y.; Wang, X.; Li, X.; Alston, B.M.; Li, B.; Clowes, R. A mobile robotic chemist. *Nature* **2020**, *583*, 237–241. [CrossRef]
94. Maleki, H.; Bertola, V. Recent advances and prospects of inkjet printing in heterogeneous catalysis. *Catal. Sci. Technol.* **2020**, *10*, 3140–3159. [CrossRef]
95. Luévano-Hipólito, E.; Torres-Martínez, L.M. Ink-jet printing films of molybdates of alkaline earth metals with scheelite structure applied in the photocatalytic CO_2 reduction. *J. Photochem. Photobiol. A* **2019**, *368*, 15–22. [CrossRef]
96. Chen, L.; Yang, C.; Xiao, Y.; Yan, X.; Hu, L.; Eggersdorfer, M.; Chen, D.; Weitz, D.; Ye, F. Millifluidics, microfluidics, and nanofluidics: Manipulating fluids at varying length scales. *MT Nano* **2021**, *16*, 100136. [CrossRef]
97. Jun, M.; Kwak, C.; Lee, S.Y.; Joo, J.; Kim, J.M.; Im, D.J.; Cho, M.K.; Baik, H.; Hwang, Y.J.; Kim, H. Microfluidics-Assisted Synthesis of Hierarchical Cu_2O Nanocrystal as C_2-Selective CO_2 Reduction Electrocatalyst. *Small Methods* **2022**, *6*, 2200074. [CrossRef]
98. Sun, Z.; Wu, B.; Ren, Y.; Wang, Z.; Zhao, C.X.; Hai, M.; Weitz, D.A.; Chen, D. Diverse Particle Carriers Prepared by Co-Precipitation and Phase Separation: Formation and Applications. *ChemPlusChem* **2021**, *86*, 49–58. [CrossRef] [PubMed]
99. Angelo, L.; Girleanu, M.; Ersen, O.; Serra, C.; Parkhomenko, K.; Roger, A.-C. Catalyst synthesis by continuous coprecipitation under micro-fluidic conditions: Application to the preparation of catalysts for methanol synthesis from CO_2/H_2. *Catal. Today* **2016**, *270*, 59–67. [CrossRef]
100. Handoko, A.D.; Wei, F.; Yeo, B.S.; Seh, Z.W. Understanding heterogeneous electrocatalytic carbon dioxide reduction through operando techniques. *Nat. Catal.* **2018**, *1*, 922–934. [CrossRef]
101. Cao, X.; Tan, D.; Wulan, B.; Hui, K.; Hui, K.; Zhang, J. In situ characterization for boosting electrocatalytic carbon dioxide reduction. *Small Methods* **2021**, *5*, 2100700. [CrossRef]
102. Zhang, B.; Zhang, J.; Shi, J.; Tan, D.; Liu, L.; Zhang, F.; Lu, C.; Su, Z.; Tan, X.; Cheng, X. Manganese acting as a high-performance heterogeneous electrocatalyst in carbon dioxide reduction. *Nat. Commun.* **2019**, *10*, 1–8. [CrossRef] [PubMed]
103. Zhang, L.; Shi, W.; Zhang, B. A review of electrocatalyst characterization by transmission electron microscopy. *J. Energy Chem.* **2017**, *26*, 1117–1135. [CrossRef]
104. Zhu, Y.; Wang, J.; Chu, H.; Chu, Y.-C.; Chen, H.M. In situ/operando studies for designing next-generation electrocatalysts. *ACS Energy Lett.* **2020**, *5*, 1281–1291. [CrossRef]
105. Vavra, J.; Shen, T.H.; Stoian, D.; Tileli, V.; Buonsanti, R. Real-time monitoring reveals dissolution/redeposition mechanism in copper nanocatalysts during the initial stages of the CO_2 reduction reaction. *Angew. Chem. Int. Ed.* **2021**, *133*, 1367–1374. [CrossRef]
106. Sakamoto, N.; Nishimura, Y.F.; Nonaka, T.; Ohashi, M.; Ishida, N.; Kitazumi, K.; Kato, Y.; Sekizawa, K.; Morikawa, T.; Arai, T. Self-assembled cuprous coordination polymer as a catalyst for CO_2 electrochemical reduction into C_2 products. *ACS Catal.* **2020**, *10*, 10412–10419. [CrossRef]
107. Baruch, M.F.; Pander, J.E., III; White, J.L.; Bocarsly, A.B. Mechanistic insights into the reduction of CO_2 on tin electrodes using in situ ATR-IR spectroscopy. *ACS Catal.* **2015**, *5*, 3148–3156. [CrossRef]
108. Rosser, T.E.; Windle, C.D.; Reisner, E. Electrocatalytic and Solar-Driven CO_2 Reduction to CO with a Molecular Manganese Catalyst Immobilized on Mesoporous TiO_2. *Angew. Chem. Int. Ed.* **2016**, *128*, 7514–7518. [CrossRef]
109. Guo, Y.; He, X.; Su, Y.; Dai, Y.; Xie, M.; Yang, S.; Chen, J.; Wang, K.; Zhou, D.; Wang, C. Machine-learning-guided discovery and optimization of additives in preparing Cu catalysts for CO_2 reduction. *J. Am. Chem. Soc.* **2021**, *143*, 5755–5762. [CrossRef]
110. Hossain, M.N.; Chen, S.; Chen, A. Thermal-assisted synthesis of unique Cu nanodendrites for the efficient electrochemical reduction of CO_2. *Appl. Catal. B* **2019**, *259*, 118096. [CrossRef]
111. Clark, E.L.; Bell, A.T. Direct observation of the local reaction environment during the electrochemical reduction of CO_2. *J. Am. Chem. Soc.* **2018**, *140*, 7012–7020. [CrossRef]

112. Zeng, L.; Shi, J.; Chen, H.; Lin, C. Ag Nanowires/C as a Selective and Efficient Catalyst for CO_2 Electroreduction. *Energies* **2021**, *14*, 2840. [CrossRef]
113. Frey, M.; Romero, T.; Roger, A.-C.; Edouard, D. Open cell foam catalysts for CO_2 methanation: Presentation of coating procedures and in situ exothermicity reaction study by infrared thermography. *Catal. Today* **2016**, *273*, 83–90. [CrossRef]
114. Kondratyuk, P.; Gumuslu, G.; Shukla, S.; Miller, J.B.; Morreale, B.D.; Gellman, A.J. A microreactor array for spatially resolved measurement of catalytic activity for high-throughput catalysis science. *J. Catal.* **2013**, *300*, 55–62. [CrossRef]
115. Lai, Y.; Jones, R.J.; Wang, Y.; Zhou, L.; Gregoire, J.M. Scanning electrochemical flow cell with online mass spectroscopy for accelerated screening of carbon dioxide reduction electrocatalysts. *ACS Comb Sci.* **2019**, *21*, 692–704. [CrossRef] [PubMed]